Published in final edited form as:
J Neurosci Res. 2014 September ; 92(9): 1143–1154. doi:10.1002/jnr.23388.

Live Cell Imaging Reveals Differential Modifications to Cytoplasmic Dynein Properties by Phospho- and Dephospho-mimic Mutations of the Intermediate Chain 2C S84

Kiev R. Blasier[*], **Michael K. Humsi**[*], **Junghoon Ha**, **Mitchell W. Ross**, **W. Russell Smiley**, **Nirja A. Inamdar**, **David J. Mitchell**, **Kevin W.-H. Lo**, and **K. Kevin Pfister**
Department of Cell Biology PO BOX 800732, School of Medicine, University of Virginia, Charlottesville VA 22908

Abstract

Cytoplasmic dynein is a multi-subunit motor protein responsible for intracellular cargo transport toward microtubule minus ends. There are multiple isoforms of the dynein intermediate chain (DYNC1I, IC) which is encoded by two genes. One way to regulate cytoplasmic dynein is by IC phosphorylation. The IC-2C isoform is expressed in all cells and the functional significance of phosphorylation on IC-2C serine 84 was investigated using live cell imaging of fluorescent protein-tagged wild type IC-2C (WT) and phospho- and dephospho-mimic mutant isoforms in axonal transport model systems. Both mutations modulated dynein functional properties. The dephospho-mimic mutant IC-2C S84A had greater co-localization with mitochondria than IC-2C wild-type (WT) or the phospho-mimic mutant IC-2C S84D. The dephospho-mimic mutant IC-2C S84A was also more likely to be motile than the phospho-mimic mutant IC-2C S84D or IC-2C WT. In contrast, the phospho-mimic mutant IC-2C S84D mutant was more likely to move in the retrograde direction than was the IC-2C S84A mutant. The phospho-mimic IC-2C S84D was also as likely as IC-2C WT to co-localize with mitochondria. Both the S84D phospho- and S84A, dephospho-mimic mutants were found to be capable of microtubule minus end directed (retrograde) movement in axons. They were also observed to be passively transported in the anterograde direction. These data suggest that the IC-2C S84 has a role in modulating dynein properties.

Keywords

cytoskeleton; motor protein; axonal transport; cytoplasmic dynein

Introduction

Membranous organelles and other cargos are transported to specific locations in cells by the microtubule-based motor proteins, cytoplasmic dynein and the kinesin family members (Akhmanova and Hammer 2010; Saxton and Hollenbeck 2012; Vallee et al. 2004).

Address correspondence to: K. Kevin Pfister, Ph.D., Cell Biology Department, PO BOX 800732, School of Medicine, University of Virginia, Charlottesville VA 22908, Phone: 434 924 1912; FAX: 434 982-3912, kkp9w@virginia.edu.
[*]These two authors contributed equally to the work.

However, much remains to be learned about the mechanisms that regulate and co-ordinate the dynein and the kinesins so that different cargos are delivered to the correct locations (Hirokawa et al. 2010; Kardon and Vale 2009). Neuronal axons offer several advantages for investigations into the regulation of organelle transport. Axons have a uniform microtubule polarity with their plus ends oriented toward axon tips (Baas et al. 1988). The kinesin family members, most of which move toward microtubule plus ends are responsible for anterograde transport toward the axon tip; while cytoplasmic dynein, which moves to microtubule minus ends, is responsible for retrograde transport toward cell bodies (Brady et al. 1982; Hirokawa et al. 2010; Kardon and Vale 2009). Long thin axons are also ideal for live cell imaging and analysis of fluorescent-protein tagged cargo and motor protein movement (Ha et al. 2008; Kaether et al. 2000; Kumar et al. 2001; Nakata et al. 1998; Pilling et al. 2006; Silverman et al. 2001; Zhang et al. 2013; Zhou et al. 2001).

Cytoplasmic dynein is a large multi-subunit complex (Pfister et al. 2006). The intermediate chain (DYNC1I, IC) plays a key role as a scaffold in the dynein complex (Pfister and Lo 2012; Pfister et al. 2006). Intermediate chain dimers directly bind to at least 4 of the other 5 dynein subunits as well two putative dynein regulators, the p150 subunit of dynactin and NudE which also binds Lis1 (Lo et al. 2007; McKenney et al. 2011; Pfister and Lo 2012). In vertebrates two genes encode the intermediate chains and additional isoforms are generated by alternative splicing (Kuta et al. 2010; Myers et al. 2007; Pfister et al. 1996a; Pfister et al. 1996b; Pfister et al. 2006; Vaughan and Vallee 1995). All cells express the IC-2C isoform and it is the only isoform expressed in fibroblasts (Kuta et al. 2010; Pfister and Lo 2012; Vaughan and Vallee 1995). We previously showed that when fluorescent protein-tagged IC isoforms are expressed at low levels in cultured neurons and PC12 cells that they make effective markers for dynein's location in axons (Ha et al. 2008; Mitchell et al. 2012; Zhang et al. 2013). Using live cell imaging of fluorescent phospho-state mutants we demonstrated that phosphorylation of IC-2C on S81 and IC-1B on S80 enhanced dynein binding to signaling endosomes, without changing dynein kinetics (Mitchell et al. 2012).

The first IC phosphorylation site identified was S84 on IC-2C, and while dominant negative studies using N-terminal regions of the IC initially suggested that phosphorylation on this site acted as a switch for binding to dynactin and thus cargo in fibroblasts, a subsequent study failed to support that model (King et al. 2003; Vaughan et al. 2001). We therefore sought use live cell imaging of fluorescent-tagged full length cytoplasmic dynein IC-2C wild type (WT), and the IC-2C S84 phospho-mimic (serine to aspartic acid, S84D) and dephospho-mimic (serine to alanine, S84A) mutations in axonal transport model systems to investigate the role of IC-2C S84 phosphorylation on dynein function and regulation. We find that the IC-2C S84 dephospho-mimic mutant is more likely to co-localize with mitochondria than WT, but that the IC-2C S84D phospho-mimic mutant has the same level of co-localization with mitochondria as WT. We also observed that the IC-2C S84A dephospho-mimic mutation has increased motility relative to WT or the phospho-mutant. Interestingly, the IC-2C S84D phospho-mimic mutation has an increased bias for retrograde movement, while the dephospho-mutant has the same anterograde bias in transport direction as was observed for WT. These results indicate that phosphorylation of IC-2C on S84 does not function simply as a switch for dynein binding to cargo. Rather, the results suggest S84 may be involved in modulating several of cytoplasmic dynein's functional properties.

Materials and Methods

Mutation of IC-2C S84

Point mutations were introduced into wild type IC-2C to produce phospho- and dephospho-mimic (serine 84 to aspartic acid, S/D, and serine 84 to alanine, S/A) mutants using the QuikChange II Site-Directed Mutagenesis Kit from Stratagene (Agilent Technologies). The resulting PCR products were transformed in XL1-Blue Supercompetent Cells and sequenced to confirm the mutation. IC-2C S84A was generated using the PCR primers 5′-CTCCATCCGCCAAGTCGG-3′ and 5′-CCGACTTGGCGGATGGAG-3′ and for IC-2C S84D the primers were 5′-CTCCATCCGACAAGTCGG-3′ and 5-′CCGACTTGTCGGATGGAG-3′.

Cell culture

Rat embryonic hippocampal neurons (E18-19) were cultured and transfected as described (Mitchell et al. 2012). For siRNA mediated reduction in the expression of IC-2, hippocampal neurons in suspension were transfected with siRNA oligonucleotides to the UTR regions of IC-2 using electroporation with the Rat Neuron Kit and setting O-030 (Lonza). There was an ~90% reduction in the level of endogenous IC-2 in the neurons treated with siRNA (Mitchell et al. 2012) and data not shown. Neurons grown on coverslips for 3–5 days *in vitro* (DIV) were transfected with fluorescent-tagged proteins for live cell imaging using the $CaPO_4$ for Mammalian Cells Transfection Kit (Clontech) and the method of (Jiang and Chen 2006). Rat pheochromocytoma, PC12, cells were cultured in DMEM (Invitrogen), 5 % FBS, and 10% FCS (all from Hyclone), with sodium pyruvate and gentimycin (Invitrogen). To obtain PC12 cells expressing low levels of the mRFP-IC-2C isoforms, cells were transfected with the mRFP-IC-2C WT or mutant plasmids using Lipofectamine2000 following the instructions of the manufacturer (Invitrogen); cells with expression of the plasmids were selected with G418 (Invitrogen). Colonies surviving drug selection were subcultured by limiting dilution and screened for low level expression of mRFP-IC-2C isoforms by live cell fluorescence microscopy. While there was no expression of fluorescent IC in approximately half of the cells, the rest of the cells had low levels of expression. PC12 cells were differentiated by growing the cells on poly-L-lysine coated coverslips in serum free media with the addition of nerve growth factor (NGF) as described (Ha et al. 2008; Myers et al. 2007). For siRNA mediated reduction in the expression of IC-2, PC12 cells in suspension were transfected with siRNA oligonucleotides to the UTR regions of IC-2 using electroporation with Kit V and setting O-029 (Ha et al. 2008) (Lonza). Approximately 85% reduction of the endogenous pool of IC was observed (data not shown). Mouse catecholaminergic (CAD) neurons were maintained in DMEM: F12 media containing 8% FBS and 1% penicillin-streptomycin and then grown on coverslips in DMEM: F12 containing 50 ng/ml sodium selenite (Qi et al. 1997), transfected on day 3 with Lipofectamine 2000, and imaged on day 4.

Live cell imaging

Co-localization of dynein intermediate chain isoforms tagged with mRFP and GFP-mito (a marker for mitochondria) was accomplished using hippocampal neurons as described (Mitchell et al. 2012). The neurons plated on coverslips were transfected by calcium

phosphate with fluorescent-protein plasmids on DIV 3 and imaged on DIV 4. Movies of puncta in living axons were collected using a 100X lens (na 1.4), and a QuantEM camera (Photometrics) on an Olympus IX81 microscope equipped with a 94% neutral density filter and external exciter and emission filter wheels. A DualView (Photometrics) was used to simultaneously project the light emitted from the red and green fluorescent proteins on to different sides of the camera chip. Exposure times were 500 ms in streaming mode with no binning. The images from each side of the chip were aligned and superimposed with the Splitview analytic module (MetaMorph7), with manual verification of the alignment relative to either the fluorescent axon or a separate DIC image of the axon. Individual puncta were manually identified in each color channel of the combined image. Co-localization of the puncta was determined by sequentially turning off the display of one color at a time for every puncta. Dynein puncta that only partially overlapped with mitochondria puncta were not scored as co-localized.

For motility analyses, catecholaminergic (CAD) neurons grown on coverslips were transfected with the fluorescent intermediate chain isoforms and imaged as described (Ha et al. 2008). Movies were collected with a 100X lens (na 1.4) on a Nikon Diaphot for 10–20s in streaming mode with 2 × 2 binning using a CoolSnapEs camera (Photometrics). Exposure times were 0.25 s. Discrete movements for each moving puncta between each pair of movie frames were tracked manually with MetaMorph. The velocity and other kinetic parameters were calculated from the tracking data as per (Ha et al. 2008). All motility is defined as any measurable puncta movement between two frames. Excursive motility is defined as a puncta moving at least one pixel (a pixel was 0.138μm) for at least 4 consecutive frames. Motile fluorescent dynein puncta were spots with 2–3 bright pixels. Kymographs of the dynein moving in the axons were made using MetaMorph.

Quantification of dynein in growth cones

Differentiated PC12 cells expressing the mRFP-IC-2C WT, IC-2C S84A or IC-2C S84D mutants were grown on coverslips and fixed in 4% formaldehyde and processed for fluorescence microscopy as described previously (Lo et al. 2007; Myers et al. 2007). Coverslips were imaged the next day with a Nikon Diaphot TMD microscope equipped with a 100X lens (na 1.4), external exciter and emission filter wheels, and internal dichroic filters for mRFP (Chroma). Single fluorescence and phase images were collected with a QuantEM camera (Photometrics) controlled with MetaMorph. An extension from the cell body was determined to be a process if it was longer than it was wide. The growth cones were at the very ends of the processes and began when the processes started to widen as determined in the fluorescence and phase images. Growth cones and cell bodies were outlined using the trace region feature in MetaMorph and their areas and fluorescence intensities were recorded. The intensity per unit area for each growth cone and its cell body were calculated. To correct for variability in the expression of the fluorescent IC isoforms between cells, the intensity per unit area for each growth cone was divided by the intensity per unit area of its cell body.

Results

The previous investigations into the role of IC-2C S84 phosphorylation for dynein function used a dominant negative approach based on over-expression of N-terminal regions, of WT and phospho-mutant isoforms in fibroblasts, which express only IC-2C (King et al. 2003; Vaughan et al. 2001). The IC N-termini lack the WD repeats and so do not bind the heavy chains (DYNC1H) or incorporate into dynein complexes (Habura et al. 1999). We have shown that, when expressed at low levels, fluorescent-tagged full length ICs incorporate into functional dynein complexes and that, in axons, the dynein is localized to small discreet fluorescent puncta of 1–3 pixels (Ha et al. 2008; Mitchell et al. 2012; Zhang et al. 2013). We therefore sought to use live cell imaging of full length IC isoforms expressed at low levels in axonal model systems to characterize the differences between the properties of dynein complexes containing the IC-2C WT and S84 phospho-mutant isoforms.

We first sought to examine the role of IC-2C S84 phosphorylation for dynein association with membranous cargos by comparing the level of co-localization of fluorescent tagged full length IC-2C wild type (WT) and IC-2C S84A (dephospho-mimic) and IC-2C S84D (phospho-mimic) with a cargo organelle, mitochondria. Mitochondria were chosen because we earlier showed that, in axons, dynein complexes containing the different IC isoforms move specific organelle cargoes and mitochondria are the only axonal cargo identified, so far, that are more likely to associate with IC-2 than IC-1 (Ha et al. 2008; Mitchell et al. 2012). In addition, the expression level of the endogenous IC-2 was reduced with IC-2 siRNA to reduce the possibility that the endogenous IC pool would suppress potential phenotypes (Ha et al. 2008; Mitchell et al. 2012).

In axons, the fluorescent IC-2C S84 mutants were localized to small fluorescent puncta of 1–3 pixels that were indistinguishable from the fluorescent IC-2C WT puncta, Figure 1 and see previous images in (Ha et al. 2008; Mitchell et al. 2012; Zhang et al. 2013). When the amount of co-localization of the IC isoforms with mitochondria was compared, it was found that the IC-2C S84A dephospho-mimic mutant, was ~2 fold more likely to co-localize with mitochondria than the IC-2C S84D phospho-mimic mutant or WT (Figure 1A). However, no significant difference was observed when the extent of co-localization of IC-2C WT and IC-2C S84D with mitochondria were compared. These observations show that the dephospho-mutant has enhanced binding to this cargo, although the phospho-mimic mutant was not blocked from binding to the cargo.

We next sought to determine if the IC-2C S84 phosphorylation state affected dynein-based transport in axons. Small puncta were also observed when the fluorescent IC-2C wild type (WT) or the IC-2C S84 phospho-mimic mutant isoforms were imaged in axons of mouse catecholaminergic neurons; although more dynein puncta were observed per unit axon length when compared to hippocampal neurons (not shown). We found that puncta of either of the two mutant intermediate chains capable of movement in both the anterograde and retrograde directions in axons (Figure 2B). The bidirectional movement of the dynein puncta demonstrated that neither of the IC-2C S84 mutants prevented active dynein transport in the retrograde direction, nor did they prevent passive dynein transport in the anterograde direction associated with cargos moved by kinesin(s).

Examination of the videos suggested that dynein puncta containing IC-2C S84A isoform were more likely to be moving than the IC-2C WT or IC-2C S8D puncta. We therefore characterized the kinetic parameters of the mutant dynein in more detail. We quantified general motility in two ways. All motility is defined as any displacement of a puncta, even if it was only for one pixel between 2 frames. When all motility of dynein with different IC isoforms was compared, we observed that the dephospho-mimic (IC-2C S84A) mutant was significantly more likely to be moving than the phospho-mimic IC-2C S84D mutant or IC-2C WT, and that the phospho-mimic IC-2C S84D mutant was as likely to be moving as IC-2C WT (Figure 3A, and Table I). Excursive motility is defined as the movement of a puncta for at least 1 pixel in each of 4 consecutive frames, and the dephospho-mimic mutant IC-2C S84A also showed significantly more excursive motility than IC-2C WT (Figure 3B).

We previously showed that there was a bias in the direction of dynein movement in the axon that favors the anterograde direction. Addition of NGF to PC12 cells leads to an increase in the relative number of dynein puncta moving in the retrograde direction, demonstrating that the directional bias of dynein movement can be regulated (Ha et al. 2008). We therefore determined if the phospho-state mutations of IC-2C S84 would alter the bias between the amount of dynein which is passively transported as cargo in the anterograde direction and the amount actively moving in the retrograde direction. We compared the length of time the dynein puncta in each axon spent moving in the anterograde and retrograde directions. We observed that dynein puncta containing the IC-2C S84D mutant spent significantly more time moving in the retrograde direction than the WT or IC-2C S84A mutant Figure 4A). Dynein puncta containing the IC-2C WT and IC-2C S84A mutant isoforms spent similar lengths of time moving in the retrograde direction (Figure 4A). There was no significant difference in the time the IC-2C isoforms spent moving in the anterograde direction (Figure 4B). However, these IC-2C S84D containing dynein puncta spent less time stationary that WT (Figure 4C). We also quantified the sum all movements made by the puncta imaged for each of the IC isoforms and compared the percentage of those in the anterograde and retrograde directions (Figure 4D). This analysis also shows that IC-2C WT and IC-2C S84A were more likely to be moving in the anterograde direction; while, IC-2C S84D was significantly more likely to move in the retrograde direction than either IC-2C WT or IC-2C S84A.

When the velocity distributions for dynein puncta containing each of the three IC isoforms were compared, it was observed that the IC-2C WT dynein had more slow retrograde movements than did dynein containing either mutant intermediate chain (Figure 5A). Comparison of the mean velocities of the different isoforms confirmed those observations (Table II). There were significant increases in the mean retrograde velocities of dynein puncta containing either IC-2C S84A or IC-2C S84D mutants relative to the IC-2C WT. We also compared the distance traveled per retrograde excursion and the time spent paused (Table 2). Dynein puncta containing either the IC-2C S84A or S84D mutants traveled farther in each of their retrograde excursions than did IC-2C WT dynein. However, there were no significant differences in the pause times between excursions when dynein puncta containing the two mutants were compared to wild type. Thus, mutating IC-2C S84 to either an alanine or aspartic acid resulted in a net increase in two key dynein motor properties, velocity and processivity, distance traveled per retrograde excursion.

The velocities of the dynein puncta when they are passively transported toward the tip of axons were also compared. We found that the anterograde transport velocity of dynein puncta containing the two mutants increased when compared to wild type dynein (Figure 5B and Table 2). In addition, the anterograde excursion distance of dynein puncta containing either the IC-2C S84A or S84D mutants increased relative to the IC-2C WT. As was observed for retrograde movement, dynein puncta containing the two mutants showed no significant differences in the pause times between anterograde excursions when compared to wild type.

Finally we determined if the differences in properties observed for the two phospho-mimic mutants relative to WT were correlated with a change in the distribution of dynein in neural cell processes. We utilized an assay based on our previous finding that cytoplasmic dynein accumulates in growth cones of differentiated PC12 cells (Figure 6A) and (Myers et al. 2007) and see (Abe et al. 2008; Grabham et al. 2007). We determined if phospho-state mutations of IC-2C S84 so modified the equilibrium of dynein movement as to alter the amount of dynein accumulation in the growth cone. Three PC12 cell lines with cells expressing low levels of the fluorescent-tagged IC-2C WT, IC-2C S84A and S84D mutants were examined. When the amounts of fluorescent dynein in growth cones from the three cell lines were compared, it was observed that both cell lines expressing the mutant IC isoforms had small but significantly reduced levels of dynein in the growth cones compared to the cell line expressing IC-2C WT (Figure 6B). Similar results were obtained when the endogenous cellular IC-2C pool was reduced with siRNA (Figure 6C) (Ha et al. 2008). These data demonstrate that the changes in dynein properties which occur when IC-2C S84 is mutated to either alanine or aspartic acid do alter the equilibrium distribution of dynein in neurites.

Discussion

Phosphorylation has long been implicated as one of the mechanisms involved in the regulation of cytoplasmic dynein (Addinall et al. 2001; Dillman and Pfister 1994; Karki et al. 1997; Kumar et al. 2000; Lin et al. 1994; Niclas et al. 1996; Salata et al. 2001). Recent studies have provided good evidence that phosphorylation of the intermediate chains is involved in dynein regulation, in particular regulating dynein binding to, and transport of membranous cargo (Mitchell et al. 2012; Vaughan et al. 2001; Whyte et al. 2008). IC-2C S84 was the first phosphorylation site identified in the cytoplasmic dynein IC (Vaughan et al. 2001). In that study a solid phase binding assay indicated that the phospho-mimic IC-2C S84D mutants bound to the p150 subunit of dynactin with lower affinity than IC-2C WT or the dephospho-mimic mutant IC-2C S84A. Also, over-expression of N-terminal regions of the dephospho-mimic mutant in cultured Cos7 cells had a greater dominant negative effect on dynein-based positioning of Golgi and endosomes than WT or the phospho-state mimic regions. These data led to a model that phosphorylation of IC-2C S84 acts as a switch, with phosphorylation blocking the dynein IC binding to the p150 subunit of dynactin and thus to membrane bounded organelle cargo, preventing dynein from moving organelles to their proper position. Alternatively, a subsequent study found no differences between WT and S84 mutant IC isoform binding to p150 in solution (King et al. 2003). The second study also reported that, when N-terminal IC-2C regions containing IC-2C WT and the two mutations were expressed in HeLa cells, the IC-2C S84A and IC-2C WT regions had almost equally

severe effects on the distribution of several endo-membranes, while the S84D mutation had a less severe phenotype (King et al. 2003).

We previously demonstrated that live cell imaging using full length fluorescent protein-tagged IC isoforms as markers for dynein complexes was an effective method to characterize the role of dynein with different IC isoforms in axons (Ha et al. 2008; Mitchell et al. 2012; Myers et al. 2007; Zhang et al. 2013). For example, we found that neurotrophin stimulated phosphorylation of IC-2C S81 (and the conserved site in IC-1B, S80) was important for cytoplasmic dynein binding to signaling endosomes but not mitochondria. We therefore used that approach in this study to investigate the role of IC-2 S84 phosphorylation in axonal cytoplasmic dynein function.

When we compared the properties of dynein containing fluorescent IC-2C WT and the two IC-2C S84 mutants in axons, we found that both the mutants had properties that differed from those of the IC-2C WT. Dynein containing the IC-2C S84A mutant had significantly greater co-localization with a known cargo of IC-2C dynein, mitochondria, than either the IC-2C S84D mutant or the IC-2C WT. Assuming that the mutants are faithful mimics of the two S84 phosphorylation states, these results suggest that dynein with dephosopho-IC-2C S84 is more likely to bind to cargo than dynein containing phospho-IC-2C S84D. However, given that the dynein with phospho-IC had the same amount of co-localization as that with IC-2C WT, it cannot be concluded that S84 phosphorylation blocks dynein binding to cargo.

Puncta containing either the IC-2C S84A or S84D mutants were also capable of bidirectional movement in axons. However, the fluorescent mutant ICs did have different properties. Puncta with the S84A mutant were more likely to be moving than those containing either IC-2C WT or the IC-2C S84D mutant. While dynein containing IC-2C S84D mutant was more likely to be moving in the retrograde direction than that with the other two isoforms. Consistent with our previous observations in PC12 cells and hippocampal neurons, IC-2C WT was more likely to move in the anterograde direction, and similar results were observed for the IC-2C S84A mutant (Ha et al. 2008; Mitchell et al. 2012). Assuming the mutants act as faithful phospho-state mimics, these data raise the possibility that phosphorylation on IC-2C S84 could act as modulating mechanism, either favoring net cargo motility in the anterograde direction (dephospho IC-2C S84) or favoring increased transport in the retrograde direction (phospho IC-2C S84). Since the dephospho-IC-2C S84 has increased motility with a directional bias toward anterograde transport, it may be the preferred conformation when the axon requires extra material for growth or repair. Alternatively, during homeostasis, or to remove material from the axon, dynein complexes with phospho-IC-2C S84 with an increased bias for retrograde transport would be used. We had previously observed an increased bias for dynein movement in the retrograde direction when NGF was applied to PC12 cells (Ha et al. 2008). It is tempting to speculate that this was due to NGF stimulation of IC-2C S84 phosphorylation through a yet to be identified signaling pathway. However, substantial further investigation will be necessary to determine if this hypothesis is correct. It is also tempting to speculate that the increased binding to cargo observed with IC-2C S84A is connected to the increased motility observed for puncta containing IC-2C S84A. It might be expected that if more dynein is bound to cargo there would be increased movement of the cargo.

We also observed that the two IC-2C S84 mutations had similar effects on the kinetics of dynein. Dynein puncta containing either mutation had increased velocities and run lengths relative to IC-2C WT, both when they function as the motor for retrograde transport and when they are cargo moved in the anterograde direction. This observation is in contrast to our previous report that dynein complexes containing phospho-mimic mutants of IC-1B S80 had no significant differences in kinetic properties when compared to WT (Mitchell et al. 2012). The finding, that both S84 mutants had increased velocity and run length, suggests that the phosphorylation state of IC-2C S84 does not regulate these properties. Interestingly, the observation that velocity and run length were increased in both directions suggests the possibility that a mechanism coordinating the dynein and kinesin family motors was altered by mutating IC-2C S84. There is considerable evidence for coordination between dynein and the kinesin family of motors *in vivo* (Ally et al. 2009; Brady et al. 1990; Gross et al. 2002; Hendricks et al. 2010; Martin et al. 1999; Pilling et al. 2006; Shubeita et al. 2008; Waterman-Storer et al. 1997). When genetic mutations are used to manipulate the number of active kinesin molecules in *Drosophila*, changes to dynein activity are also observed (Martin et al. 1999; Shubeita et al. 2008). It has also been reported that neuronal dynein activity can be modulated to allow for changes in cargo load (Mallik et al. 2004; Yi et al. 2011). If the effect of both mutations of the IC-2C S84 is to slightly increase the number of engaged dynein complexes on the cargo for retrograde transport, then coordination between the anterograde and retrograde motors might be predicted to result in a compensatory increase in the number of active kinesin molecules and the observed increases in anterograde velocity and run length. If this model is correct, it is possible that the predicted increased number of engaged dynein complexes was the result of a greater over-expression of the two mutant IC-2C isoforms relative to the level of fluorescent IC-2C WT. However we consider this to be unlikely for several reasons. All three isoforms were in identical plasmids, except for the mutated codon, and the transfections were performed under identical conditions. So there is no reason to expect differential expression of the isoforms. Also the results from several transfections were pooled during the analysis of each isoform, which should mitigate any possible differences in expression level in individual experiments. Finally, no kinetic differences were observed in similar experiments when over expressed WT IC-1 and IC-2 were compared, or when two S80 phospho-state mimic mutants were compared to WT (Ha et al. 2008; Mitchell et al. 2012).

Both mutant IC-2C isoforms were less likely to accumulate in growth cones than IC-2C WT, even in the presence of endogenous IC-2. With the several changes in dynein properties caused by the mutations it is difficult to assign direct mechanisms or combinations of mechanisms to explain the altered equilibrium. The reduced dynein accumulation observed with IC-2C S84D is most easily explained by the increased probability of retrograde movement for this isoform. Alternatively, perhaps the increased velocity and run lengths observed for both mutants, in both directions, was sufficient to change the equilibrium level of dynein in the growth cone.

Assuming that the mutants are faithful mimics for the different phosphorylation states of S84, the data presented here characterizing the motility of dynein complexes with wild type and mutant IC-2C S84 in axons, suggests that S84 phosphorylation does just not function as

an off switch for dynein motility. Rather, our data suggest a model in which different phosphorylation states act to fine tune cytoplasmic dynein properties. However, even if the mutations do not accurately mimic the effects of S84 phosphorylation, these data show that mutating the IC -2C serine 84 to either alanine or aspartic acid has effects on dynein function and thus the data provide insight to potential dynein regulatory mechanisms.

Acknowledgments

This work was supported by a grant from the NIH Institute of General Medical Science: RO1 GM086472 to K.K.P.

We thank Dr. Robert Bloodgood for critical reading of initial versions of the manuscript.

References

Abe TK, Honda T, Takei K, Mikoshiba K, Hoffman-Kim D, Jay DG, Kuwano R. Dynactin is essential for growth cone advance. Biochemical and biophysical research communications. 2008; 372(3): 418–422. [PubMed: 18477476]

Addinall SG, Mayr PS, Doyle S, Sheehan JK, Woodman PG, Allan VJ. Phosphorylation by cdc2-CyclinB1 kinase releases cytoplasmic dynein from membranes. The Journal of biological chemistry. 2001; 276(19):15939–15944. [PubMed: 11278950]

Akhmanova A, Hammer JA 3rd. Linking molecular motors to membrane cargo. Current opinion in cell biology. 2010; 22(4):479–487. [PubMed: 20466533]

Ally S, Larson AG, Barlan K, Rice SE, Gelfand VI. Opposite-polarity motors activate one another to trigger cargo transport in live cells. J Cell Biol. 2009; 187(7):1071–1082. [PubMed: 20038680]

Baas PW, Deitch JS, Black MM, Banker GA. Polarity orientation of microtubules in hippocampal neurons: uniformity in the axon and nonuniformity in the dendrite. Proceedings of the National Academy of Sciences of the United States of America. 1988; 85(21):8335–8339. [PubMed: 3054884]

Brady ST, Lasek RJ, Allen RD. Fast axonal transport in extruded axoplasm from squid giant axon. Science. 1982; 218(4577):1129–1131. [PubMed: 6183745]

Brady ST, Pfister KK, Bloom GS. A monoclonal antibody against kinesin inhibits both anterograde and retrograde fast axonal transport in squid axoplasm. Proceedings of the National Academy of Sciences of the United States of America. 1990; 87(3):1061–1065. [PubMed: 1689058]

Dillman JF 3rd, Pfister KK. Differential phosphorylation in vivo of cytoplasmic dynein associated with anterogradely moving organelles. J Cell Biol. 1994; 127(6 Pt 1):1671–1681. [PubMed: 7528220]

Grabham PW, Seale GE, Bennecib M, Goldberg DJ, Vallee RB. Cytoplasmic dynein and LIS1 are required for microtubule advance during growth cone remodeling and fast axonal outgrowth. The Journal of neuroscience: the official journal of the Society for Neuroscience. 2007; 27(21):5823–5834. [PubMed: 17522326]

Gross SP, Welte MA, Block SM, Wieschaus EF. Coordination of opposite-polarity microtubule motors. J Cell Biol. 2002; 156(4):715–724. [PubMed: 11854311]

Ha J, Lo KW, Myers KR, Carr TM, Humsi MK, Rasoul BA, Segal RA, Pfister KK. A neuron-specific cytoplasmic dynein isoform preferentially transports TrkB signaling endosomes. J Cell Biol. 2008; 181(6):1027–1039. [PubMed: 18559670]

Habura A, Tikhonenko I, Chisholm RL, Koonce MP. Interaction mapping of a dynein heavy chain. Identification of dimerization and intermediate-chain binding domains. The Journal of biological chemistry. 1999; 274(22):15447–15453. [PubMed: 10336435]

Hendricks AG, Perlson E, Ross JL, Schroeder HW 3rd, Tokito M, Holzbaur EL. Motor coordination via a tug-of-war mechanism drives bidirectional vesicle transport. Current biology: CB. 2010; 20(8):697–702. [PubMed: 20399099]

Hirokawa N, Niwa S, Tanaka Y. Molecular motors in neurons: transport mechanisms and roles in brain function, development, and disease. Neuron. 2010; 68(4):610–638. [PubMed: 21092854]

Jiang M, Chen G. High Ca2+-phosphate transfection efficiency in low-density neuronal cultures. Nature protocols. 2006; 1(2):695–700.

Kaether C, Skehel P, Dotti CG. Axonal membrane proteins are transported in distinct carriers: a two-color video microscopy study in cultured hippocampal neurons. Molecular biology of the cell. 2000; 11(4):1213–1224. [PubMed: 10749925]

Kardon JR, Vale RD. Regulators of the cytoplasmic dynein motor. Nature reviews Molecular cell biology. 2009; 10(12):854–865.

Karki S, Tokito MK, Holzbaur EL. Casein kinase II binds to and phosphorylates cytoplasmic dynein. The Journal of biological chemistry. 1997; 272(9):5887–5891. [PubMed: 9038206]

King SJ, Brown CL, Maier KC, Quintyne NJ, Schroer TA. Analysis of the dynein-dynactin interaction in vitro and in vivo. Molecular biology of the cell. 2003; 14(12):5089–5097. [PubMed: 14565986]

Kumar S, Lee IH, Plamann M. Cytoplasmic dynein ATPase activity is regulated by dynactin-dependent phosphorylation. The Journal of biological chemistry. 2000; 275(41):31798–31804. [PubMed: 10921911]

Kumar S, Zhou Y, Plamann M. Dynactin-membrane interaction is regulated by the C-terminal domains of p150(Glued). EMBO reports. 2001; 2(10):939–944. [PubMed: 11571270]

Kuta A, Deng W, Morsi El-Kadi A, Banks GT, Hafezparast M, Pfister KK, Fisher EM. Mouse cytoplasmic dynein intermediate chains: identification of new isoforms, alternative splicing and tissue distribution of transcripts. PloS one. 2010; 5(7):e11682. [PubMed: 20657784]

Lin SX, Ferro KL, Collins CA. Cytoplasmic dynein undergoes intracellular redistribution concomitant with phosphorylation of the heavy chain in response to serum starvation and okadaic acid. J Cell Biol. 1994; 127(4):1009–1019. [PubMed: 7962066]

Lo KW, Kogoy JM, Pfister KK. The DYNLT3 light chain directly links cytoplasmic dynein to a spindle checkpoint protein, Bub3. The Journal of biological chemistry. 2007; 282(15):11205–11212. [PubMed: 17289665]

Mallik R, Carter BC, Lex SA, King SJ, Gross SP. Cytoplasmic dynein functions as a gear in response to load. Nature. 2004; 427(6975):649–652. [PubMed: 14961123]

Martin M, Iyadurai SJ, Gassman A, Gindhart JG Jr, Hays TS, Saxton WM. Cytoplasmic dynein, the dynactin complex, and kinesin are interdependent and essential for fast axonal transport. Molecular biology of the cell. 1999; 10(11):3717–3728. [PubMed: 10564267]

McKenney RJ, Weil SJ, Scherer J, Vallee RB. Mutually exclusive cytoplasmic dynein regulation by NudE-Lis1 and dynactin. The Journal of biological chemistry. 2011; 286(45):39615–39622. [PubMed: 21911489]

Mitchell DJ, Blasier KR, Jeffery ED, Ross MW, Pullikuth AK, Suo D, Park J, Smiley WR, Lo KW, Shabanowitz J, Deppmann CD, Trinidad JC, Hunt DF, Catling AD, Pfister KK. Trk Activation of the ERK1/2 Kinase Pathway Stimulates Intermediate Chain Phosphorylation and Recruits Cytoplasmic Dynein to Signaling Endosomes for Retrograde Axonal Transport. The Journal of neuroscience: the official journal of the Society for Neuroscience. 2012; 32(44):15495–15510. [PubMed: 23115187]

Myers KR, Lo KW, Lye RJ, Kogoy JM, Soura V, Hafezparast M, Pfister KK. Intermediate chain subunit as a probe for cytoplasmic dynein function: Biochemical analyses and live cell imaging in PC12 cells. Journal of neuroscience research. 2007; 85(12):2640–2647. [PubMed: 17279546]

Nakata T, Terada S, Hirokawa N. Visualization of the dynamics of synaptic vesicle and plasma membrane proteins in living axons. J Cell Biol. 1998; 140(3):659–674. [PubMed: 9456325]

Niclas J, Allan VJ, Vale RD. Cell cycle regulation of dynein association with membranes modulates microtubule-based organelle transport. J Cell Biol. 1996; 133(3):585–593. [PubMed: 8636233]

Pfister, KK.; Lo, KW-H. Cytoplasmic Dynein Function Defined by Subunit Composition. In: King, SM., editor. Dyneins. London: Academic Press; 2012. p. 424-439.

Pfister KK, Salata MW, Dillman JF 3rd, Torre E, Lye RJ. Identification and developmental regulation of a neuron-specific subunit of cytoplasmic dynein. Molecular biology of the cell. 1996a; 7(2):331–343. [PubMed: 8688562]

Pfister KK, Salata MW, Dillman JF 3rd, Vaughan KT, Vallee RB, Torre E, Lye RJ. Differential expression and phosphorylation of the 74-kDa intermediate chains of cytoplasmic dynein in

cultured neurons and glia. The Journal of biological chemistry. 1996b; 271(3):1687–1694. [PubMed: 8576170]

Pfister KK, Shah PR, Hummerich H, Russ A, Cotton J, Annuar AA, King SM, Fisher EM. Genetic analysis of the cytoplasmic dynein subunit families. PLoS genetics. 2006; 2(1):e1. [PubMed: 16440056]

Pilling AD, Horiuchi D, Lively CM, Saxton WM. Kinesin-1 and Dynein are the primary motors for fast transport of mitochondria in Drosophila motor axons. Molecular biology of the cell. 2006; 17(4):2057–2068. [PubMed: 16467387]

Qi Y, Wang JK, McMillian M, Chikaraishi DM. Characterization of a CNS cell line, CAD, in which morphological differentiation is initiated by serum deprivation. The Journal of neuroscience: the official journal of the Society for Neuroscience. 1997; 17(4):1217–1225. [PubMed: 9006967]

Salata MW, Dillman JF 3rd, Lye RJ, Pfister KK. Growth factor regulation of cytoplasmic dynein intermediate chain subunit expression preceding neurite extension. Journal of neuroscience research. 2001; 65(5):408–416. [PubMed: 11536324]

Saxton WM, Hollenbeck PJ. The axonal transport of mitochondria. Journal of cell science. 2012; 125(Pt 9):2095–2104. [PubMed: 22619228]

Shubeita GT, Tran SL, Xu J, Vershinin M, Cermelli S, Cotton SL, Welte MA, Gross SP. Consequences of motor copy number on the intracellular transport of kinesin-1-driven lipid droplets. Cell. 2008; 135(6):1098–1107. [PubMed: 19070579]

Silverman MA, Kaech S, Jareb M, Burack MA, Vogt L, Sonderegger P, Banker G. Sorting and directed transport of membrane proteins during development of hippocampal neurons in culture. Proceedings of the National Academy of Sciences of the United States of America. 2001; 98(13): 7051–7057. [PubMed: 11416186]

Vallee RB, Williams JC, Varma D, Barnhart LE. Dynein: An ancient motor protein involved in multiple modes of transport. J Neurobiol. 2004; 58(2):189–200. [PubMed: 14704951]

Vaughan KT, Vallee RB. Cytoplasmic dynein binds dynactin through a direct interaction between the intermediate chains and p150Glued. J Cell Biol. 1995; 131(6 Pt 1):1507–1516. [PubMed: 8522607]

Vaughan PS, Leszyk JD, Vaughan KT. Cytoplasmic dynein intermediate chain phosphorylation regulates binding to dynactin. The Journal of biological chemistry. 2001; 276(28):26171–26179. [PubMed: 11340075]

Waterman-Storer CM, Karki SB, Kuznetsov SA, Tabb JS, Weiss DG, Langford GM, Holzbaur EL. The interaction between cytoplasmic dynein and dynactin is required for fast axonal transport. Proceedings of the National Academy of Sciences of the United States of America. 1997; 94(22): 12180–12185. [PubMed: 9342383]

Whyte J, Bader JR, Tauhata SB, Raycroft M, Hornick J, Pfister KK, Lane WS, Chan GK, Hinchcliffe EH, Vaughan PS, Vaughan KT. Phosphorylation regulates targeting of cytoplasmic dynein to kinetochores during mitosis. J Cell Biol. 2008; 183(5):819–834. [PubMed: 19029334]

Yi JY, Ori-McKenney KM, McKenney RJ, Vershinin M, Gross SP, Vallee RB. High-resolution imaging reveals indirect coordination of opposite motors and a role for LIS1 in high-load axonal transport. J Cell Biol. 2011; 195(2):193–201. [PubMed: 22006948]

Zhang J, Twelvetrees AE, Lazarus JE, Blasier KR, Yao X, Inamdar NA, Holzbaur EL, Pfister KK, Xiang X. Establishing a novel knock-in mouse line for studying neuronal cytoplasmic dynein under normal and pathologic conditions. Cytoskeleton (Hoboken). 2013; 70(4):215–227. [PubMed: 23475693]

Zhou HM, Brust-Mascher I, Scholey JM. Direct visualization of the movement of the monomeric axonal transport motor UNC-104 along neuronal processes in living Caenorhabditis elegans. The Journal of neuroscience: the official journal of the Society for Neuroscience. 2001; 21(11):3749–3755. [PubMed: 11356862]

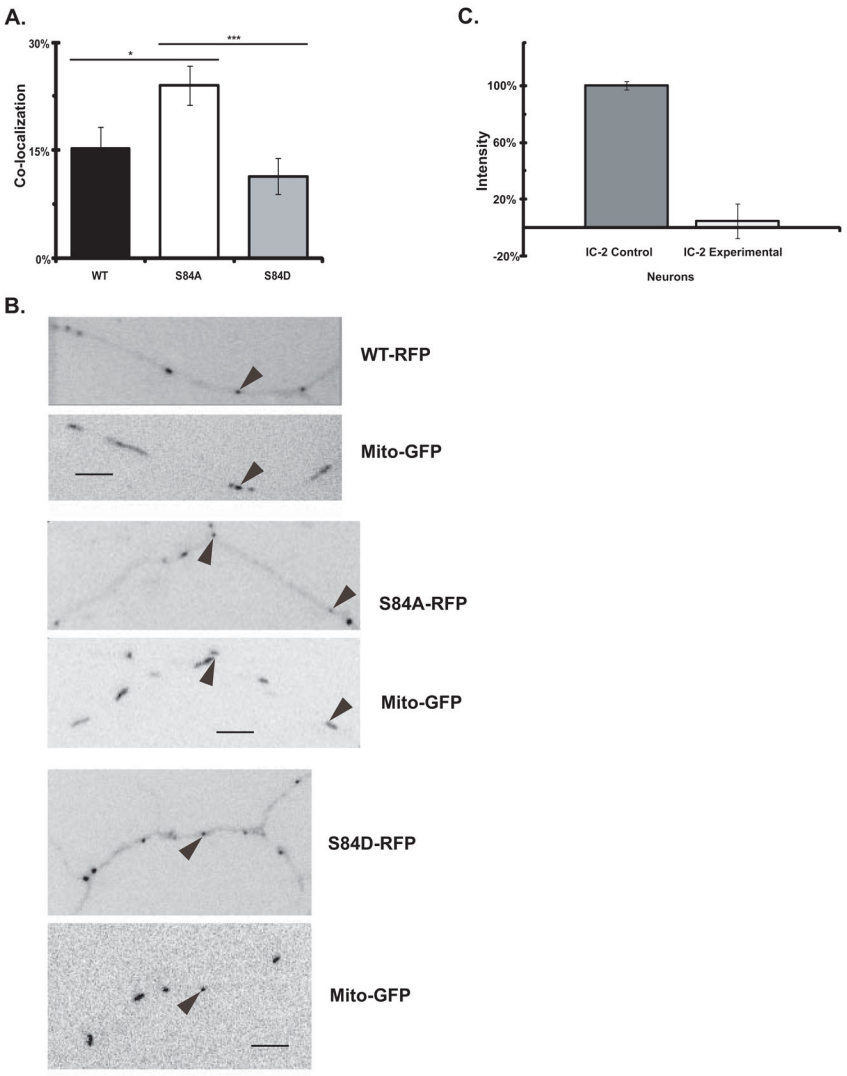

Figure 1. Comparison of the co-localization of dynein IC-2C WT and phospho-state IC-2C mutations with mitochondria

Rat embryonic hippocampal neurons were transfected with IC-2 siRNA oligonucleotides by Lonza nucelofection prior to plating and then co-transfected with Mito-GFP and the indicated dynein IC-2C isoform tagged with mRFP on DIV 3 by $CaPO_4$. Axons of living cells were imaged the next day.

A. The IC-2C S84A dephospho-mimic mutation enhances dynein co-localization with mitochondria. The amount of co-localization of the indicated isoform with mitochondria was determined by imaging axons of living cells in the two colors simultaneously with a Dualview. The number of puncta in each color and the number that overlap were quantified and the percentage of dynein puncta that co-localized with mitochondria was graphed. WT (**black**), IC-2C WT, (n = 216 dynein, 346 mitochondria, and 31 co-localizing); S84A (**white**), IC-2C S84A, (n = 287 dynein, 395 mitochondria, and 64 co-localizing; S84D (**gray**), IC-2C S84D (n = 310 dynein, 445 mitochondria, annd 36 co-localizing). There were significant differences in co-localization between the WT and S84A isoforms, and between

the S84A and S84D isoforms, * P<0.03, *** P<0.001 Student's t-test. The difference between WT and S84D was not significant.

B. Co-localization dynein IC-2C WT and mutant isoforms in cultured hippocampal neurons. Neurons were co-transfected as described and movies of axons of living cells were made with the GFP and mRFP signals collected simultaneously using DualView. The pairs of panels are from single DualView frames with the indicated IC-2C mRFP isoform (top panel of each pair) and Mito-GFP (bottom panel of each pair) signals aligned and the puncta displayed in reverse contrast. Arrows identify puncta that co-localize. Puncta that only showed partial overlap or that did not co-localize in all frames are not identified. In these examples, 15% of the IC-2C WT co-localized with mitochondria, 24% of the IC-2C S84A mutant co-localized with mitochondria, and 11% of the IC-2C S81D co-localized with mitochondria. Scale bar is 5 μm.

C. Quantitation of effect of siRNA in reducing the expression level of IC-2 isoforms in neurons. Cultured rat cortical neurons were transfected with siRNA oligonucleotides as described in the Methods and (Mitchell et al. 2012). After 4 days the cells were lysed and polypeptides resolved by SDS-PAGE and Western blotting. The blots were probed with IC-2 specific antibody (Pfister et al. 1996b; Vaughan and Vallee 1995) and the intensity of the endogenous IC-2 bands were quantified using MetaMorph. The intensities of the bands for cells transfected with control scrambled oligonucleotides and experimental siRNA oligonucleotides are graphed (n=2). A greater than 90% reduction in the expression of endogenous IC-2 was achieved.

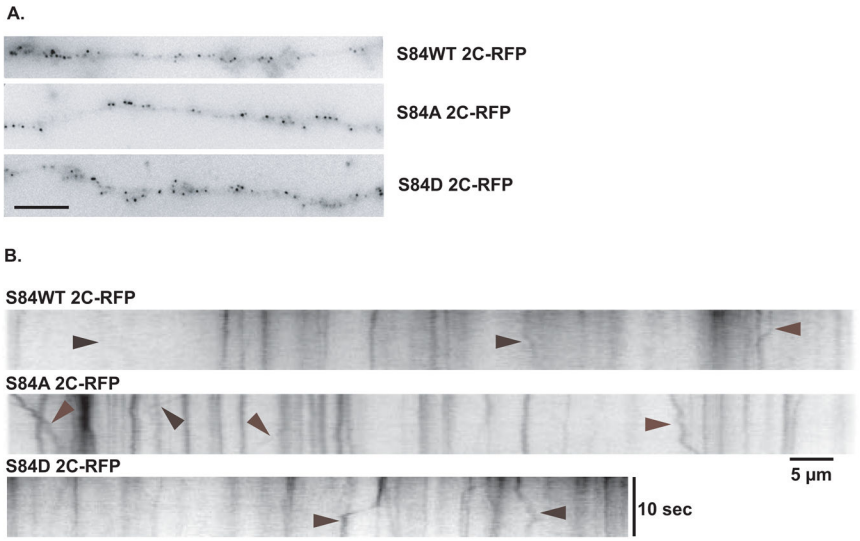

Figure 2. Live cell imaging of dynein containing IC-2C WT mRFP and the IC-2C S84A and S84D mutations in axons

Mouse catecholaminergic neurons were transfected with either the IC-2C WT mRFP, IC-2C S84A, or IC-2C S84D isoforms with Lipofectamine2000 on the 3rd day of culture and the next day fluorescent dynein was imaged in axons of living cells.

A. In axons, all three fluorescent IC isoforms are observed as small puncta. Single frame images from movies of axons of cell expressing the IC-2C or mutant isoform indicated to the right of the image. The WT, S84A and S84D IC-2C isoforms all have the appearance of small puncta in the axons. The scale bar is 5 µm.

B. Imaging bi-directional motility of dynein puncta with IC-2C WT mRFP, and the IC-2C S84A and S84D mutants in axons. Kymographs were made from movies of axons expressing the fluorescent IC-2C isoform indicated above the kymographs. Arrowheads point to the traces of dynein puncta with movement in either the anterograde or retrograde directions. The cell body is located to the left for the kymographs of the IC-2C mutants. The time and distance scales are as indicated.

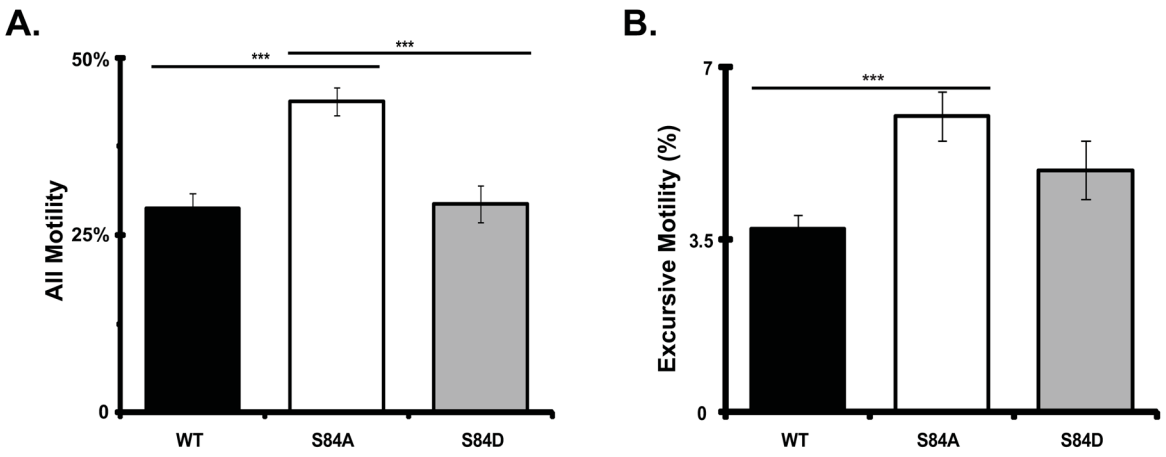

Figure 3. The dephospho-mimic mutant IC-2C S84A dynein puncta have increased motility in axons

Cytoplasmic dynein IC-2C isoforms were separately transfected into neurons and the fluorescent dynein was imaged as for Figure 2. **black,** IC-2C WT; **white,** IC-2C S84A; and **gray**, IC-2C S84D. Number of axons: WT 47, S84A 44, S84D 36; number of puncta: WT 2867, S84A 1795, S84D 2490.

A. All Motility. For each of the three IC isoforms, the percentage of moving puncta is graphed. Individual dynein puncta were scored as being motile if they showed any displacement between at least two frames. There were significant differences when the motility of S84A puncta was compared to that of the WT or S84D isoforms, *** $P<0.001$ Student's t-test. The difference between dynein puncta containing IC-2C WT and IC-2C S84D was not significant

B. Excursive Motility. For each of the three IC isoforms, the percentage of moving puncta exhibiting excursive movement is graphed. Individual dynein puncta were scored as having excursive motility if they showed displacement of at least 1 pixel for four consecutive frames. There was a significant difference when the excursive motility of dynein puncta containing the S84A was compared to that of the WT isoforms, *** $P<0.001$ Student's t-test. The differences between S84D and WT or S84A were not significant.

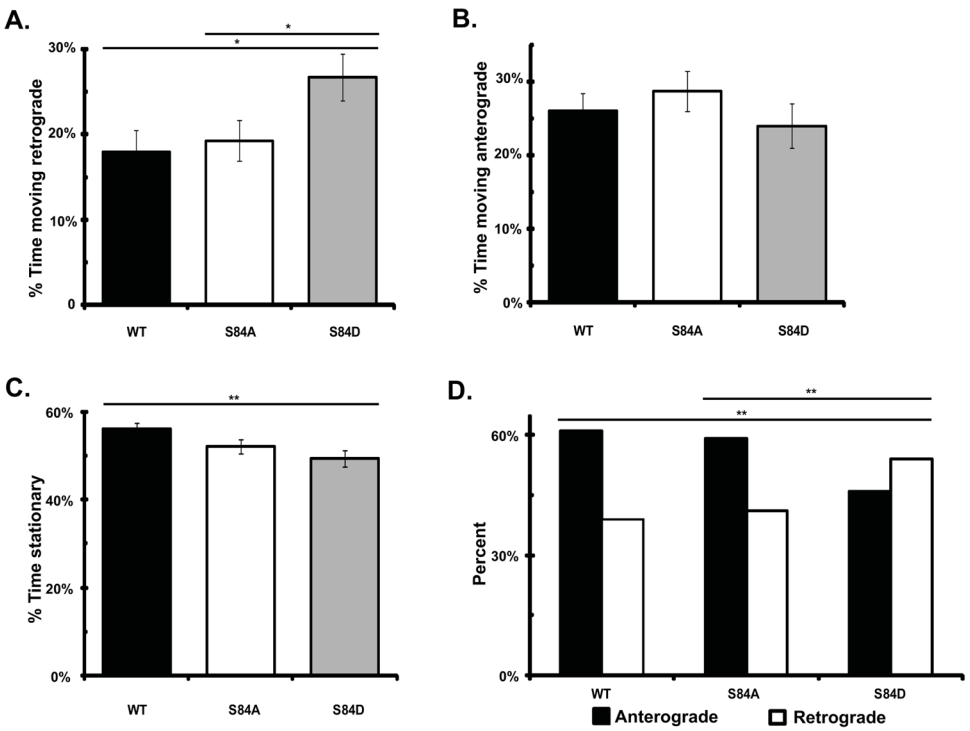

Figure 4. The phospho-mimic mutant IC-2C S84D dynein puncta have increased retrograde motility in axons

Cytoplasmic dynein IC-2C isoforms were separately transfected into neurons and the fluorescent dynein was imaged as for Figure 2.

A, B, C. For each of the three IC isoforms the time each excursive puncta in axons spent moving in the retrograde direction, (**A**), moving in the anterograde direction (**B**), and stationary (**C**) was calculated for each axon and the averages are graphed as percent, **black**, IC-2C WT; **white**,IC-2C S84A; and **gray,** IC-2C S84D. There was a significant increase in the amount of time dynein puncta containing the IC-2C S84D, phosphomimic mutant spent moving in the retrograde direction compared to that of IC-2C WT and the IC-2C S84 mutant, *P<0.02 Student's t-test. There was no significant difference between the time the WT and the S84A isoforms spent in retrograde movement. No significant differences in the time spent moving in the anterograde direction was observed when the three IC isoforms were compared. The IC-2C S84D mutant dynein puncta spent significantly less time stationary (49.3 +/− 0.02−) than did the IC-2C WT dynein isoform (56.0 =/− 0.01%), ** P< 0.01, Student's t-test. The S84A mutant was stationary 52.1 +/−0.01% of the time and this was not significantly different from that of IC-2C WT or the IC-2C S84D mutant.

D. For every excursive puncta, the direction of every movement between two frames was identified and the number in each direction for the three IC isoforms was summed and graphed as percent moving retrograde (**white**) or anterograde (**black**), IC-2C WT n = 1,758; IC-2C S84A, n = 1,953; and IC-2C S84D, n= 2017. There were significantly more IC-2C S84D movements in the retrograde direction (and fewer in the anterograde direction) than were observed for IC-2C S84 or IC-2C WT; **, P<0.01, X^2 test.

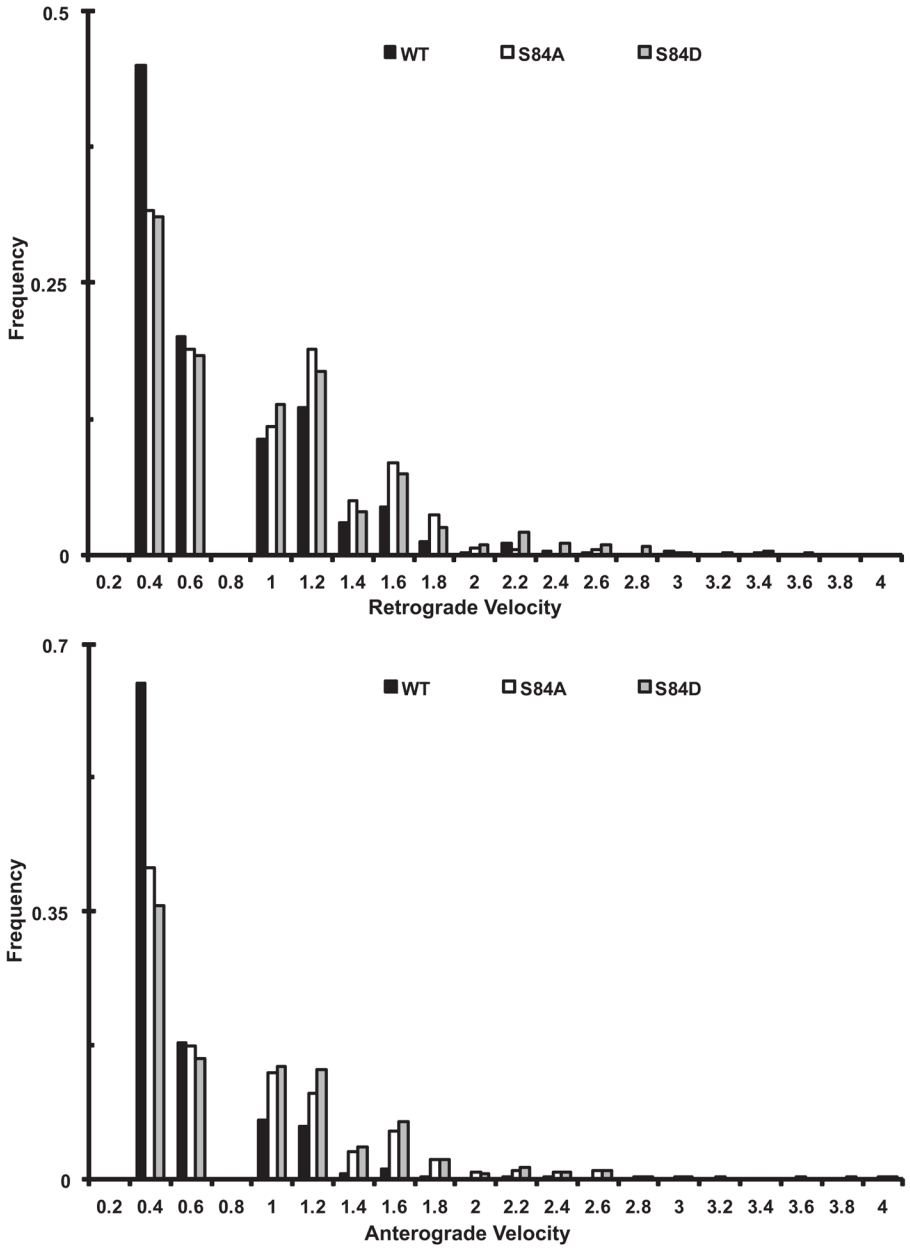

Figure 5. Comparison of the velocity distributions of dynein puncta containing wild type and mutant IC-2C isoforms in axons

Cytoplasmic dynein IC-2C isoforms were transfected into neurons and the fluorescent dynein was imaged as for Figure 2. The movements of individual puncta between each frame were tracked manually and analyzed with MetaMorph.

A. Comparison of the retrograde interval velocity distributions of the IC-2C WT and mutant isoforms in axons. Velocities (μm/s) of individual retrograde movements of GFP-IC-2C dynein puncta between two frames were plotted against the frequency of their occurrence; **black**, IC-2C WT dynein (n=684); **white** IC-2C S84A (n=780), and **gray** IC-2C S84D dynein puncta (n=1030).

B) Comparison of the anterograde interval velocity distributions of the IC-2C WT and mutant isoforms in axons/neurons. Velocities (μm/s) of individual anterograde movements of GFP-IC-2C dynein puncta between two frames were plotted against the frequency of their occurrence; **black** IC-2C WT (n=1074), **white** IC-2C S84A (n=1172), and **gray** IC-2C S84D dynein puncta (n=987).

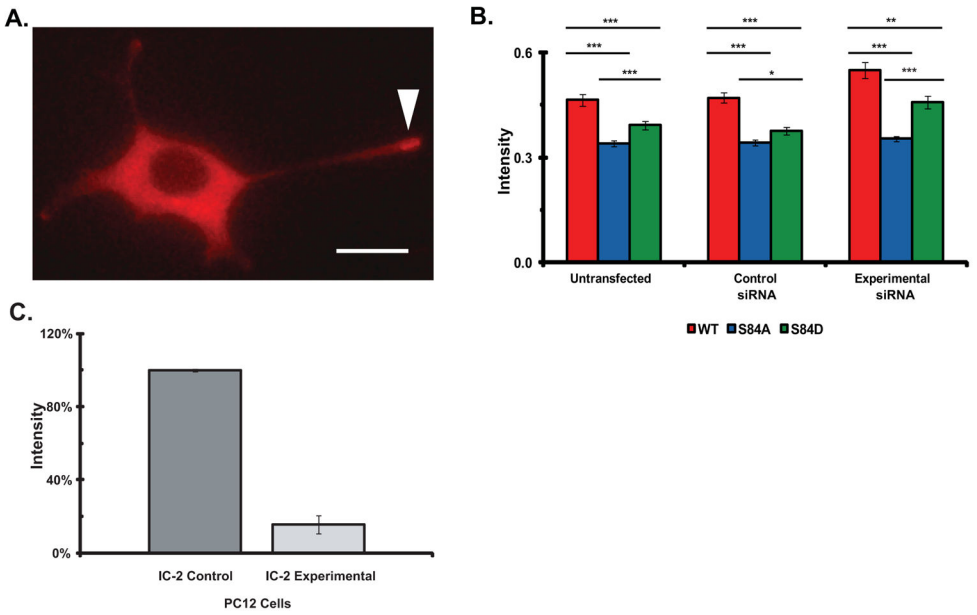

Figure 6. Mutations of IC-2C at S84 modulate dynein motility

Three PC12 cell lines with the stable expression of mRFP IC-2C WT, and the IC-2C S84A and IC-2C S84D mutations were generated. The cells were differentiated by the addition of NGF and 3–4 days later the cells and the growth cones of neurite processes of the differentiated cells were imaged.

A. Dynein distribution in differentiated PC12 cells. Representative image of mRFP IC-2C WT in differentiated PC12 cell showing dynein accumulation in a growth cone of a long process marked with arrowhead, see also Figure 3 in (Myers et al. 2007). The scale bar is 10 μm.

B. Mutation of IC-2C S84 changes dynein motility and reduces the accumulation of dynein in growth cone. The fluorescence intensity the mRFP-IC-2C in the three cell lines with stable expression of the tagged IC isoforms per unit growth cone area was measured and corrected for differences in IC-mRFP expression in the different cell bodies; **red** IC-2C WT, **blue** IC-2C S84A, and **green** IC-2C S84D. The IC isoform intensities were measured under three experimental conditions; **Untransfected**, the three parent cells lines with stable expression of the indicated IC isoform (left set of bars), **Control siRNA**, the parent cell lines transfected with the control siRNA reagent (middle set of bars), and **Experimental siRNA**, the cell lines transfected with an IC-2 siRNA reagent to reduce the expression of the endogenous IC-2 (right set of bars). There were significant differences between the fluorescent intensities which measure the accumulation of dynein in growth cones between the IC-2C WT and both mutant cell lines under all three experimental conditions. Significant differences were also observed when the dynein accumulations in cell expressing the S84A & S84D mutations were compared. (Student's t-test * $p < 0.05$, ** $p < 0.002$, and *** $P < 0.001$). Untrasfected cell lines; IC-2C WT n=84, S84A n=184, S84D n=125. Control siRNA; IC-2C WT n=112, S84A n=169, S84D n=130. Experimental siRNA; IC-2C WT n=119, S84A, n=170, S84D n=47.

C. Quantitation of effect of siRNA in reducing the expression level of IC-2 isoforms in PC12 cells. PC12 cells were transfected with siRNA oligonucleotides as described in the

Methods and (Ha et al. 2008). After 4 days the cells were lysed and polypeptides resolved by SDS-PAGE and Western blotting. The blots were probed with the 74.1 antibody and the intensities of the bands corresponding to the endogenous IC-2 were quantified using MetaMorph. The intensities of the bands for cells transfected with control scrambled oligonucleotides and experimental siRNA oligonucleotides are graphed (n=3). An ~85% reduction in the expression of endogenous IC-2 was achieved.

Table I

Motility of dynein complexes with IC-2C WT and phospho-mutants in axons of catecholaminergic neurons

Catecholaminergic neurons were transfected with the indicated IC-2C mRFP isoform and imaged the next day as described for Figure 2 and in Methods. Each dynein puncta was defined as being either stationary, exhibiting excursive movement, or exhibiting jiggling movement. Excursive movement is movement for at least 4 frames and at least 1 pixel in each frame. Jiggling movement is any movement that does not last for at least 4 frames, and could be as little as 1 pixel movement between 2 frames. The “All Motility” category graphed in Figure 3 is the sum of excursive and jiggling movement.

	IC-2C WT	IC-2C S84A	IC-2C S84D
Number of videos	47	43	35
Total puncta	2867	1795	2490
Stationary puncta	2123	1044	1869
Jiggling movement	647	650	532
Excursive movement	97	101	98
Total observation time (s)	940	860	700

Table II

Kinetics of the motility of dynein complexes with IC-2C WT and phospho-mutants in axons

Neurons were transfected with the indicated IC isoform tagged with mRFP and movies of the movement of the fluorescent dynein intermediate chains were obtained as for Figure 2. The movement kinetics for the puncta containing each IC isoform was analyzed and averaged. Interval velocities for dynein puncta with mRFP-IC-2C or mRFP-IC-1B moving in axons were calculated for every movement between each pair of movie frames and averaged. Excursions are puncta movements greater than one pixel for at least 4 frames. Excursion distance is total distance traveled per movement interval. Pauses are periods of time with no dynein movement that separate two excursions. There were no significant differences in pause time for the WT and mutant dyneins (Student's t-test).

IC-2C Isoform	WT	S84A	S84D
Retrograde Motility			
Mean Interval Velocity, μm/s[a]	0.89	1.02***	1.06***
(+/− SEM)	(0.02)	(0.02)	(0.02)
Number	683	780	1030
Excursion Distance			
Mean Distance traveled, μm[b]	1.9	2.6*	3.1***
(+/− SEM)	(0.24)	(0.19)	(0.22)
Number	55	67	79
Pause Time, sec	2.43	2.52	2.48
(+/− SEM)	(0.23)	(0.15)	(0.16)
Number	61	74	91
Anterograde Motility			
Mean Interval Velocity, μm/s[c]	0.71	0.97***	1.03***
(+/− SEM)	(0.01)	(0.02)	(0.02)
Number	1074	1172	987
Excursion Distance			
Mean Distance traveled, μm[d]	1.22	2.43***	2.28***
(+/− SEM)	(0.09)	(0.21)	(0.17)
Number	61	88	94
Pause Time sec	2.22	2.53	2.82
(+/− SEM)	(0.19)	(0.16)	(0.29)
Number	99	87	61

[a] Dynein puncta containing either mutant IC-2C have a greater interval retrograde velocity than WT, *** p<0.001, Student's t-test.

[b] Dynein puncta containing either mutant IC-2C travel greater distances per retrograde excursion than WT dynein, *** p<0.001, *p< 0.02, Student's t-test.

[c] Dynein puncta containing either mutant IC-2C have a greater interval anterograde velocity than WT, *** p<0.001, Student's T-test.

[d] Dynein puncta containing either mutant IC-2C travel greater distances per retrograde excursion than WT dynein, *** p<0.001, Student's t-test.